Supplementary Information

Benchmarking Monolayer MoS_2 and WS_2 Field-Effect Transistors

*Amritanand Sebastian[1], Rahul Pendurthi[1], Tanushree H Choudhury[2], Joan M Redwing[2,3,4] & Saptarshi Das[1,3,4]**

[1]*Deparment of Engineering Science and Mechanics, Pennsylvania State University, University Park, PA 16802*

[2]*2D Crystal Consortium-Materials Innovation Platform (2DCC-MIP), Pennsylvania State University, University Park, PA, 16802, USA*

[3]*Department of Materials Science and Engineering, Pennsylvania State University, University Park, PA 16802*

[4]*Materials Research Institute, Pennsylvania State University, University Park, PA 16802*

Supplementary Figure 1

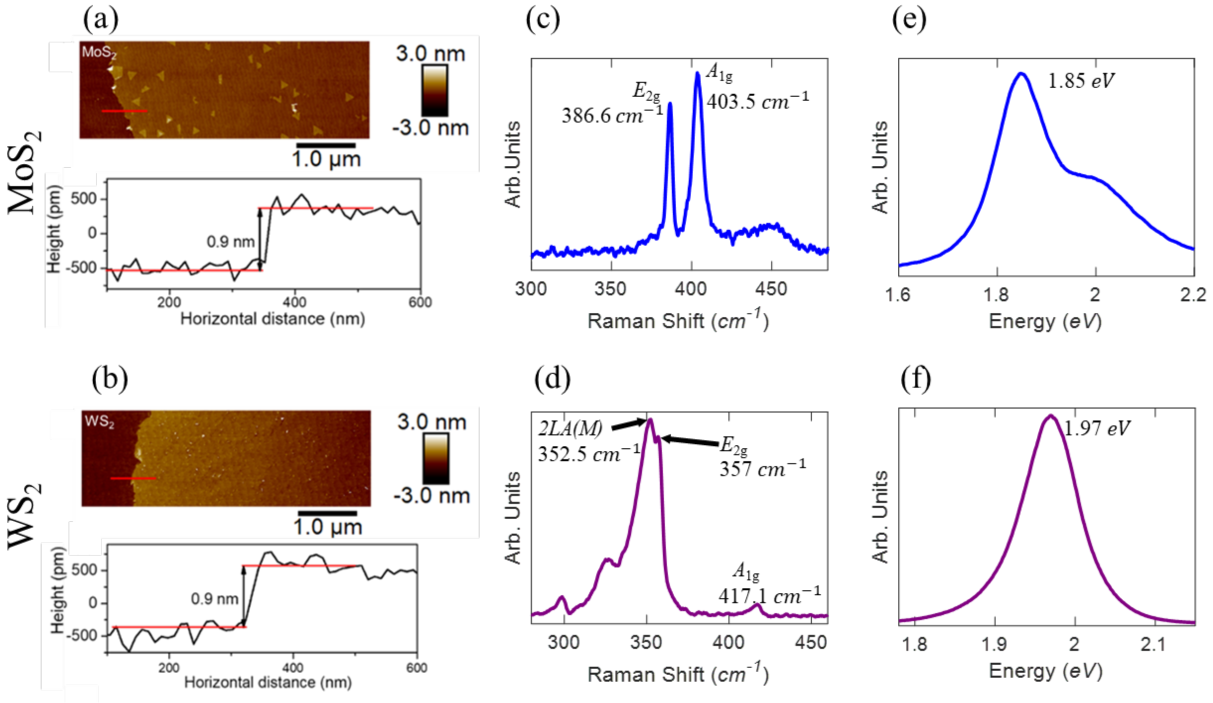

Supplementary Figure 1. Characterization of MOCVD grown monolayer WS$_2$ and MoS$_2$. AFM of scratch and height profile across the scratch along the red line for (a) MoS$_2$ and (b) WS$_2$. Raman spectrum with the characteristic peaks for c) MoS$_2$ with E_{2g} at 386.6 cm^{-1} and A_{1g} at 403.5 cm^{-1} and d) WS$_2$ with E_{2g} at 357 cm^{-1}, A_{1g} at 417.1 cm^{-1} and 2LA(M) at 352.5 cm^{-1}. PL spectrum for e) MoS$_2$ and f) WS$_2$ showing the characteristic monolayer response with peaks at 1.85 eV and 1.97 eV, respectively.

Supplementary Figure 2

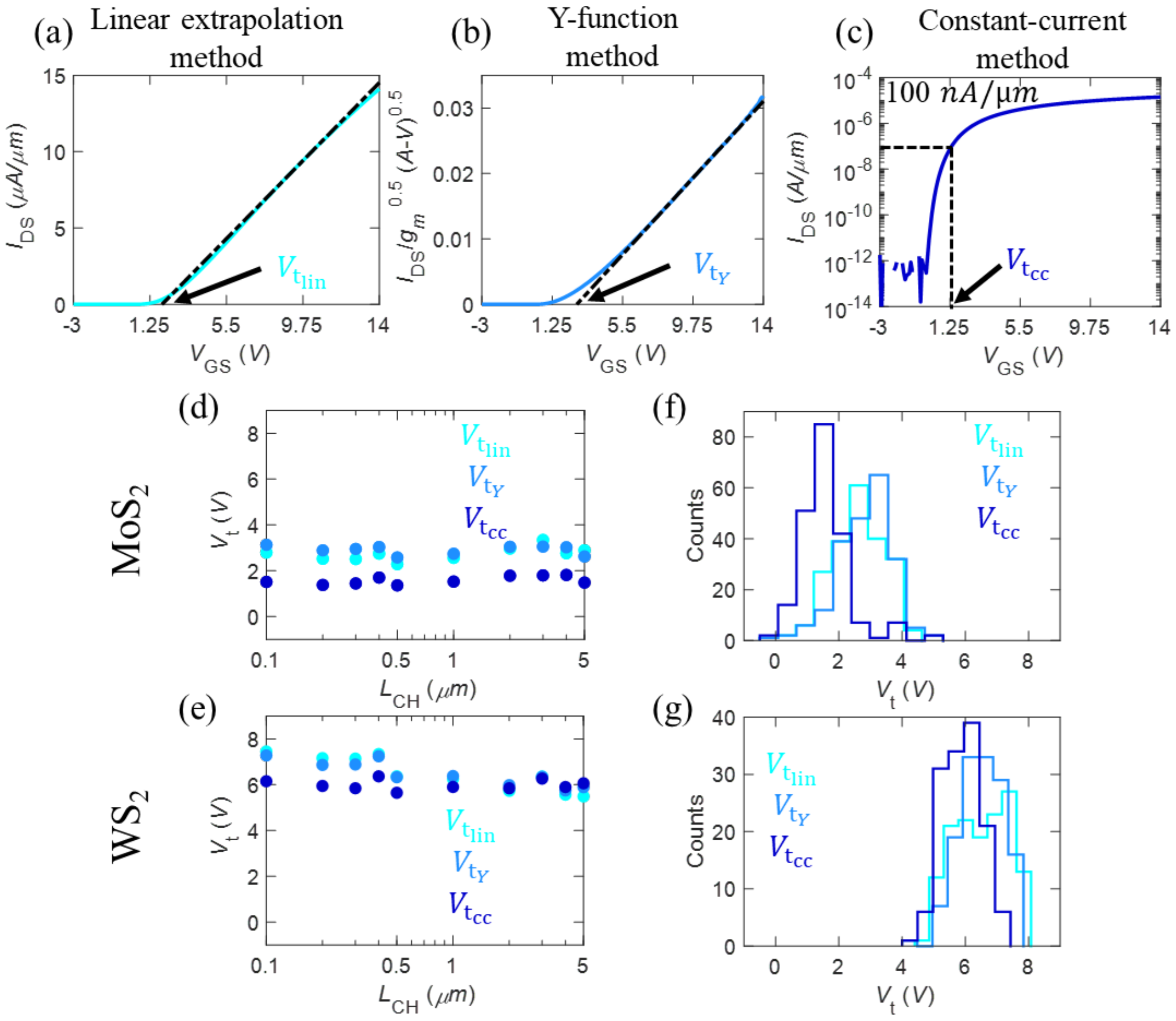

Supplementary Figure 2. Threshold voltage extraction, channel length dependence, and device to device variation. Threshold voltage extraction using a) linear extrapolation ($V_{t_{\text{lin}}}$), b) Y-function (V_{t_Y}), and c) constant-current method ($V_{t_{\text{cc}}}$). The median values for $V_{t_{\text{lin}}}$, V_{t_Y}, and $V_{t_{\text{cc}}}$ verses channel length (L_{CH}) showing no scaling effects for d) MoS_2 and e) WS_2. Histograms showing the variation in $V_{t_{\text{lin}}}$, V_{t_Y}, and $V_{t_{\text{cc}}}$ across all measured devices for f) MoS_2 and g) WS_2 FETs for different channel lengths.

Supplementary Note 1

In 2D FET literature, threshold voltage is extracted using various methods such as linear extrapolation ($V_{\mathrm{t_{lin}}}$), Y-function (V_{t_Y}), and constant-current method ($V_{\mathrm{t_{cc}}}$) as shown in Supplementary Fig. 2a-c. Linear extrapolation is the most common among these techniques. However, poor ON-state performance, presence of SB at the metal/semiconductor interface, and contact-gating effect in a back-gated geometry can limit the use of linear extrapolation. Y-function method is more appropriate for contact dominated FETs. Finally, constant current method is simply another threshold voltage extraction technique, which is discussed for completeness. Clearly none of the extracted threshold voltages, $V_{\mathrm{t_{lin}}}$, V_{t_Y}, and $V_{\mathrm{t_{cc}}}$ show any channel length (L_{CH}) dependence as evident from Supplementary Fig. 2d and 2e for MoS_2 and WS_2, respectively. Supplementary Fig. 2f and 2g show the distributions of $V_{\mathrm{t_{lin}}}$, V_{t_Y}, and $V_{\mathrm{t_{cc}}}$ for all measured MoS_2 and WS_2 FETs, respectively. For MoS_2 FETs, the distributions of V_{t_Y} and $V_{\mathrm{t_{lin}}}$ are very similar with median values of 2.9 V and 2.5 V, respectively. However, $V_{\mathrm{t_{cc}}}$ results in lower median value of 1.5 V for MoS_2, as the extraction is done at a constant current of 100 $nA/\mu m$, which is lower than the current at $V_{\mathrm{t_{lin}}}$ and V_{t_Y}. A similar trend is observed for WS_2, where both V_{t_Y} and $V_{\mathrm{t_{lin}}}$ have median values of 6.5 V and 6.4 V, while $V_{\mathrm{t_{cc}}}$ has a median value of 5.9 V. The corresponding standard deviations were found to be 0.8 V for $V_{\mathrm{t_{lin}}}$, V_{t_Y}, and $V_{\mathrm{t_{cc}}}$ for MoS_2 and 0.8 V, 0.7 V, and 0.6 V, respectively, for $V_{\mathrm{t_{lin}}}$, V_{t_Y}, and $V_{\mathrm{t_{cc}}}$, in case of WS_2. Supplementary Table 1 summarize the statistics of $V_{\mathrm{t_{lin}}}$, V_{t_Y}, and $V_{\mathrm{t_{cc}}}$

Supplementary Table 1

Device-to-device variation in threshold voltage				
	MoS_2		WS_2	
	Median, Mean ± SD	Min, Max	Median, Mean ± SD	Min, Max
$V_{\mathrm{t_{cc}}}$ (V)	1.5, 1.7 ± 0.8	-0.5, 5.3	5.9, 5.8 ± 0.6	4.2, 7.3
V_{t_Y} (V)	2.9, 2.8 ± 0.8	-0.1, 5.3	6.5, 6.5 ± 0.7	4.2, 7.8
$V_{\mathrm{t_{lin}}}$ (V)	2.5, 2.9 ± 0.8	-0.1, 4.5	6.4, 6.5 ± 0.8	4.5, 8

Supplementary Note 2

It is important to discuss the possible origin of the variation seen in the electrical characteristics of monolayer MoS_2 and WS_2 FETs. Low device-to-device variation in MoS_2 and WS_2 FETs is attributed to the MOCVD growth of single-crystalline and epitaxial monolayers on the sapphire substrates. This is confirmed by in-plane XRD phi-scans in Fig. 1e and 1f, for MoS_2 and WS_2, respectively, which show six-fold rotational symmetry and epitaxial alignment of the monolayer with the underlying sapphire. If the films were polycrystalline with a high degree of misorientation within the plane of the film, then we would expect to see multiple peaks at different angles in the in-plane XRD scan. These films were also transferred to a Quantifoil Cu grid to investigate the microstructure in TEM by using selected area diffraction pattern (SAED) and dark field imaging. As shown in detailed materials characterization of these films (https://www.mri.psu.edu/2d-crystal-consortium/user-facilities/thin-films/list-thin-film-samples-available) the respective SAED patterns show a single crystalline pattern, while composite dark field maps illuminate two contrasting regions in the monolayer films. For MoS_2 these regions correspond to anti-phase domains. For WS_2 however, the regions are unidirectional and are separated by translational boundaries. We believe that it is possible to reduce the spatial variations in 2D FETs through further optimization of growth and improvement in fabrication process flow, which is unlikely for UTB Si owing to significant thickness variations at length scales similar to monolayer MoS_2 and WS_2. In addition, random dopant fluctuations and detrimental quantum confinement effects leading to increase in the bandgap of ultra-thin Si open up opportunities for 2D materials for advanced scaling nodes.

Supplementary Figure 3

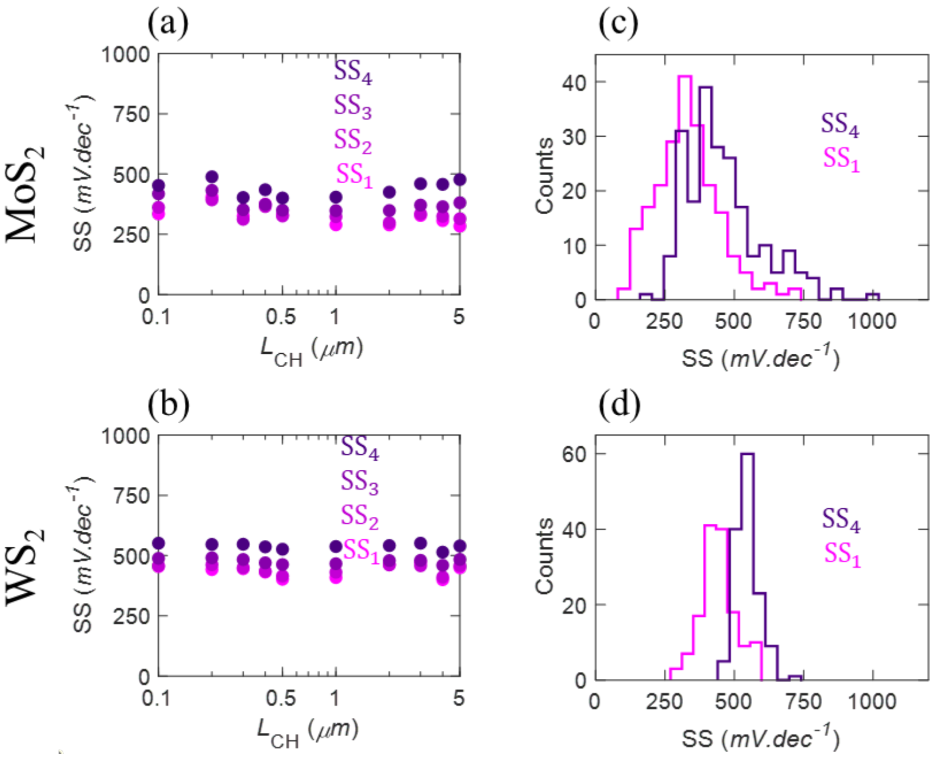

Supplementary Figure 3. Channel length dependence and device to device variation in subthreshold slope. The median subthreshold slope extracted over 1 (SS_1), 2 (SS_2), 3 (SS_3), and 4 (SS_4) orders of magnitude change in the drain current for a) MoS$_2$ and b) WS$_2$ as a function of L_{CH}. No L_{CH} dependence is observed. Histograms showing the device-to-device variation in SS_1 and SS_4 across all c) MoS$_2$ and d) WS$_2$ FETs.

Supplementary Table 2

Device-to-device variation in subthreshold slope and interface traps				
	MoS$_2$		WS$_2$	
	Median, Mean ± SD	Min, Max	Median, Mean ± SD	Min, Max
SS_1 $(mV.dec^{-1})$	327, 335 ± 115	93, 729	438, 443 ± 66	296, 596
SS_2 $(mV.dec^{-1})$	335, 344 ± 109	103, 740	449, 453 ± 56	305, 618
SS_3 $(mV.dec^{-1})$	369, 386 ± 116	124, 791	480, 483 ± 45	369, 621
SS_4 $(mV.dec^{-1})$	432, 460 ± 138	166, 1000	541, 546 ± 42	453, 738
D_{IT} $(10^{12}\ eV^{-1}cm^{-2})$	6.2, 6.6 ± 2.3	1.75, 15.7	8, 8.1 ± 0.7	6.5, 11.2

Supplementary Figure 4

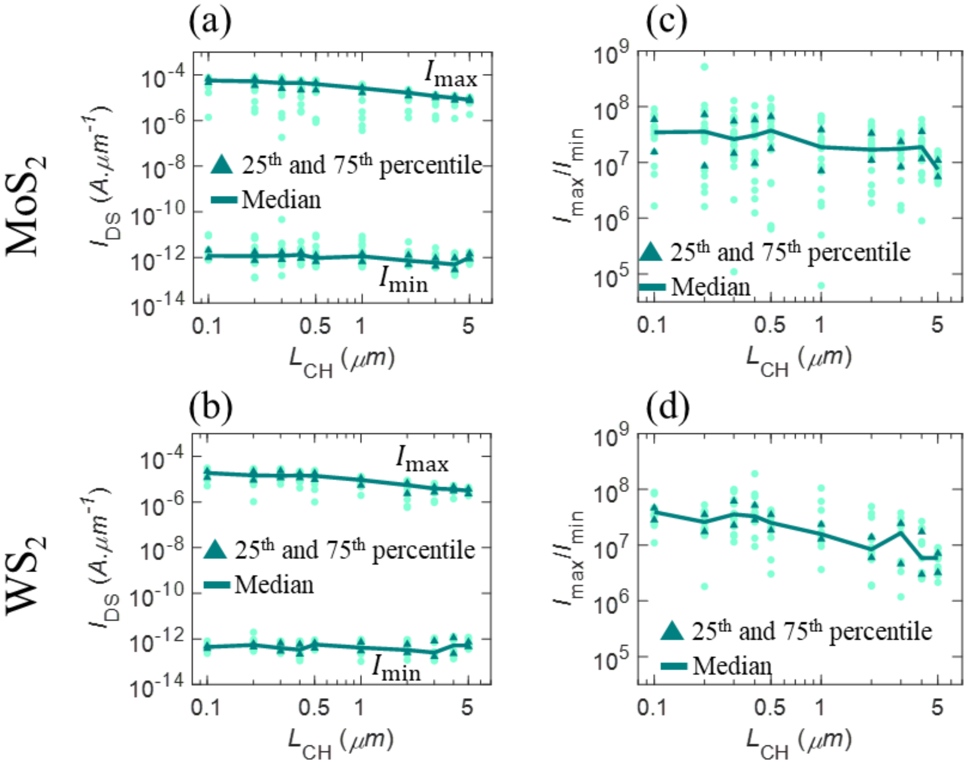

Supplementary Figure 4. Channel length dependence of maximum, minimum, and ratio of maximum to minimum current. Distribution of maximum current ($I_{\max}$) and minimum current ($I_{\min}$) for different channel lengths for a) MoS_2 and b) WS_2 FETs, extracted from the transfer characteristics. Median, 25th percentile and 75th percentile is denoted. Distribution of ratio of maximum to minimum current ratio ($I_{\max}/I_{\min}$) for different L_{CH} for c) MoS_2 and d) WS_2 FETs. $I_{\max}/I_{\min}$ is mostly found to be independent of L_{CH} for both MoS_2 and WS_2 FETs. Note that $I_{\max}$ demonstrates some L_{CH} dependence for longer channel devices with $L_{\mathrm{CH}} \geq 1$ µm for MoS_2 and WS_2 FETs due to the linear scaling law but can be ignored for $I_{\max}/I_{\min}$ which is measured in orders of magnitude.

Supplementary Table 3

Device-to-device variation in $I_{\max}/I_{\min}$				
	MoS_2		WS_2	
	Median, Mean ± SD	Min, Max	Median, Mean ± SD	Min, Max
$I_{\max}/I_{\min}$ ($\times 10^7$)	2.1, 3.4 ± 5.5	6.2×10^{-3}, 52	2.1, 2.7 ± 2.6	0.1, 19

Supplementary Table 4

Benchmarking median $I_{\max}/I_{\min}$ for L_{CH} = 100 nm				
	$I_{\max}/I_{\min}$	EOT (nm)	$V_{\text{GS,Range}}$ (V)	$SV_{\text{GS,Range}}$ (V) at SEOT = 0.9 nm
[1] - MoS_2	≈7×10^6	1.9	1.5 to -0.5 (2)	0.94
[1] - MoS_2	≈4×10^6	50	-	-
Our Work - MoS_2	3.5×10^7	22	14 to -3 (17)	0.65
Our Work - WS_2	3.9×10^7	22	12 to -5 (17)	0.65
[2] - UTB SOI	1.3×10^6	4	1.8 to -0.2 (2)	0.45

Supplementary Note 3

Mobility from peak Transconductance: The field-effect electron mobility is extracted from the transconductance (g_{m}) using Supplementary Equation (S1).

$$\mu_{g_m} = \frac{dI_{\text{DS}}}{dV_{\text{GS}}}\left(\frac{L_{\text{CH}}}{WC_{\text{OX}}V_{\text{DS}}}\right) \qquad (S1)$$

Y-function mobility: The linear part of Y-function, given by Supplementary Equation (S2) is extrapolated to obtain Y-function threshold. μ_Y is extracted using the slope of Y-function *versus* $V_{\text{GS}} - V_{\text{t}_Y}$

$$Y = \frac{I_{\text{DS}}}{\sqrt{g_{\text{m}}}} = (\mu_Y W C_{\text{OX}} V_{\text{DS}})^{0.5}(V_{\text{GS}} - V_{\text{t}_Y}) \qquad (S2)$$

TLM mobility: TLM mobility (μ_{TLM}) is obtained from the slope of the total resistance (R_{T}) *versus* L_{CH} using Supplementary Equation (S3).

$$R_{\text{T}} = 2R_{\text{c}} + R_{\text{ch}};\ R_{\text{ch}} = \frac{L_{\text{CH}}}{\mu_{\text{TLM}}C_{\text{OX}}(V_{\text{GS}} - V_{\text{t}_{\text{lin}}})} = \frac{L_{\text{CH}}}{qn_{\text{S}}\mu_{\text{TLM}}};\ n_{\text{S}} = \frac{C_{\text{OX}}(V_{\text{GS}} - V_{\text{t}_{\text{lin}}})}{q} \qquad (S3)$$

Supplementary Figure 5

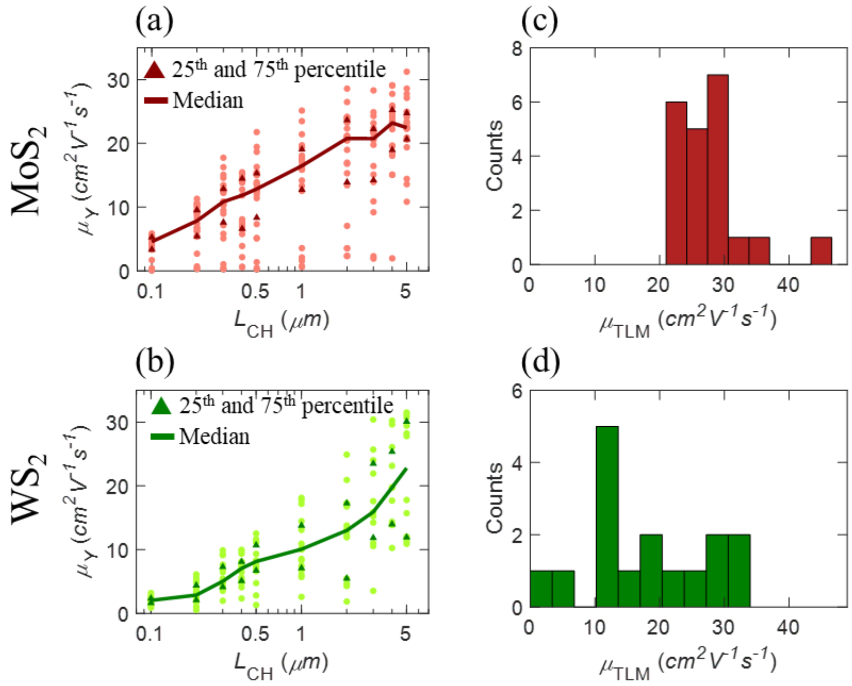

Supplementary Figure 5. Device-to-device variation in Y-function mobility and TLM mobility. The distribution of Y-function mobility (μ_Y) for different channel lengths (L_{CH}) for a) MoS$_2$ and b) WS$_2$ FETs. Median, 25th percentile and 75th percentile is denoted. The distribution of the TLM mobility (μ_{TLM}) for c) MoS$_2$ and d) WS$_2$

Supplementary Table 5

Device-to-device variation in field-effect carrier mobility								
	$\mu_{g_m}(cm^2\ V^{-1}s^{-1})$				$\mu_Y\ (cm^2\ V^{-1}s^{-1})$			
	MoS$_2$		WS$_2$		MoS$_2$		WS$_2$	
$L_{\mathrm{CH}}(\mu m)$	Median, Mean ± SD	Min, Max	Median, Mean ± SD	Min, Max	Median, Mean ± SD	Min, Max	Median, Mean ± SD	Min, Max
0.1	4, 4 ± 1	1, 5	3, 3 ± 1	2, 5	5, 4 ± 2	0.1, 6	2, 2 ± 0.6	0.9, 3
0.2	7, 7 ± 3	0.3, 11	4, 4 ± 2	1, 8	8, 7 ± 3	0.3, 11	3, 3.2 ± 2	0.6, 6
0.3	10, 9 ± 4	0.3, 15	7, 7 ± 3	3, 11	11, 10 ± 5	0.3, 18	5, 6 ± 2	2, 10
0.4	11, 9 ± 4	0.7, 15	9, 7 ± 3	2, 11	12, 10 ± 5	0.6, 16	7, 7 ± 2	2, 10
0.5	12, 11 ± 5	0.2, 18	9, 9 ± 3	1, 12	13, 12 ± 6	0.3, 22	8, 8 ± 3	1, 13

1	15, 14 ± 5	2, 23	10, 10 ± 5	2, 19	17, 14 ± 7	0.6, 25	10, 11 ± 5	3, 18
2	19, 18 ± 7	3, 26	12, 12 ± 6	2, 24	21, 18 ± 8	2, 29	13, 13 ± 7	2, 25
3	18, 20 ± 4	13, 27	18, 19 ± 7	8, 29	21, 18 ± 7	2, 28	16, 17 ± 8	4, 30
4	23, 23 ± 4	17, 28	21, 20 ± 6	12, 30	23, 22 ± 6	2, 29	20, 20 ± 7	10, 30
5	24, 24 ± 3	17, 30	29, 24 ± 9	12, 33	23, 22 ± 5	11, 31	23, 22 ± 9	11, 32

Supplementary Note 4

We have evaluated n_{S} by considering the effect of C_{IT}. After evaluating C_{IT} from the subthreshold slope, Supplementary Equation (S4) was used to evaluate n_{S} in the ON-state.

$$n_{\mathrm{S}} = \frac{C_{\mathrm{G}}}{q}\left(V_{\mathrm{GS}} - V_{t_{\mathrm{lin}}}\right); \qquad C_{\mathrm{G}} = \frac{C_{\mathrm{OX}}\,(C_{\mathrm{IT}} + C_{\mathrm{S}})}{C_{\mathrm{OX}} + C_{\mathrm{IT}} + C_{\mathrm{S}}}; \qquad C_{\mathrm{S}} = \frac{q^2\, n_{\mathrm{S}}}{k_{\mathrm{B}}T} \tag{S4}$$

Here, C_{G} is the total gate capacitance. $n_{\mathrm{S}} = 10^{13}\ cm^{-2}$ for MoS_2 and $n_{\mathrm{S}} = 4.4 \times 10^{12}\ cm^{-2}$ for WS_2 used in the main text corresponds to C_{S} of $6.13 \times 10^{-1}\ F.m^{-2}$ and $2.7 \times 10^{-1}\ F.m^{-2}$ respectively. Maximum C_{IT} is found to be $2.5 \times 10^{-2}\ F.m^{-2}$ and $1.7 \times 10^{-2}\ F.m^{-2}$ for MoS_2 and WS_2, respectively and $C_{\mathrm{OX}} = 1.6 \times 10^{-3}\ F.m^{-2}$. Hence, in the ON-state $C_{\mathrm{S}} \gg C_{\mathrm{IT}}$ as well as $C_{\mathrm{S}} \gg C_{\mathrm{OX}}$, resulting in $C_{\mathrm{G}} \approx C_{\mathrm{OX}}$, simplifying Supplementary Equation (S4) into Supplementary Equation (S5).

$$n_{\mathrm{S}} = \frac{C_{\mathrm{OX}}}{q}\left(V_{\mathrm{GS}} - V_{\mathrm{t_{lin}}}\right) \tag{S5}$$

To obtain a constant n_{S}, a constant overdrive voltage $\left(V_{\mathrm{GS}} - V_{\mathrm{t_{lin}}}\right)$ is ensured by extracting the $V_{\mathrm{t_{lin}}}$ and then estimating the required V_{GS} for every device. I_{ON} is extracted from the output characteristics with a V_{GS} step size of 2 V, and the median error in n_{S} is $0.11 \times 10^{12}\ cm^{-2}$ and $0.03 \times 10^{12}\ cm^{-2}$ for MoS_2 and WS_2 FETs, respectively. n_{S} is also found for the analysis of R_{c}. R_{c} is extracted from the transfer characteristics with a V_{GS} step size of 85 mV, and median error in n_{S} is 0.003 and $0.004 \times 10^{12}\ cm^{-2}$ for MoS_2 and WS_2 FETs, respectively.

Supplementary Table 6

Device-to-device variation in TLM mobility				
	MoS_2		WS_2	
	Median, Mean ± SD	Min, Max	Median, Mean ± SD	Min, Max
$\mu_{\mathrm{TLM}}(cm^2\ V^{-1}s^{-1})$	27.3, 27.7 ± 5.5	21.1, 46.5	16.2, 17.9 ± 9.7	2, 33.3

Supplementary Figure 6

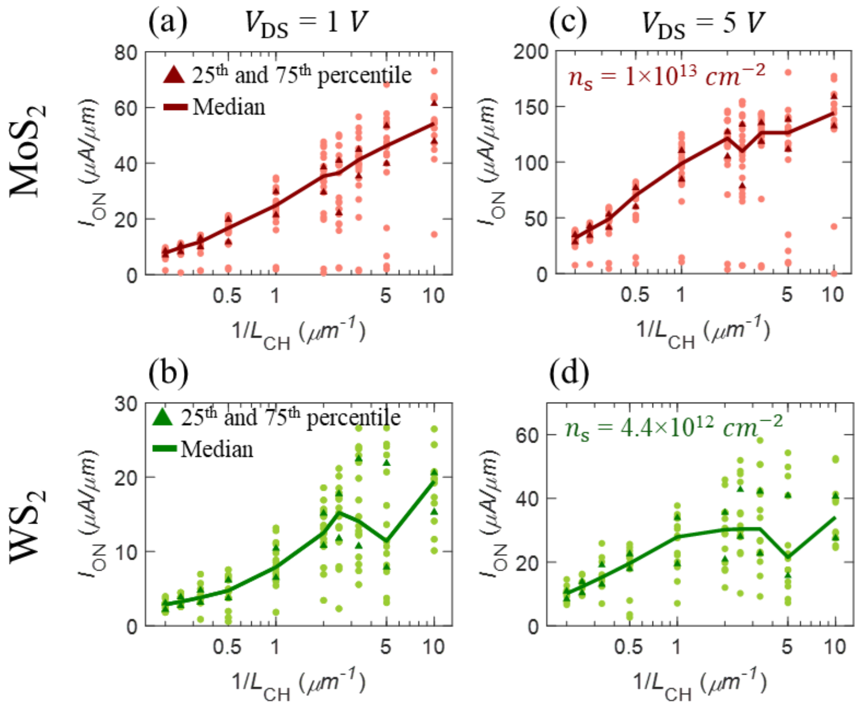

Supplementary Figure 6. Channel length dependence of drive current. Distribution of I_{ON} as a function of channel length (L_{CH}) for a) MoS_2 and b) WS_2 FETs for V_{DS} of 1 V, and for c) MoS_2 and d) WS_2 FETs for V_{DS} of 5 V. Note that the distribution is plotted as a function of $1/L_{\mathrm{CH}}$. Median, 25th percentile and 75th percentile is denoted.

Supplementary Table 7

Device-to-device variation in the drive current								
$I_{\mathrm{ON}}(\mu A.\mu m^{-1})$ at $V_{\mathrm{DS}} = 1\ V$					$I_{\mathrm{ON}}(\mu A.\mu m^{-1})$ at $V_{\mathrm{DS}} = 5\ V$			
	MoS_2		WS_2		MoS_2		WS_2	
L_{CH} (μm)	Median, Mean ± SD	Min, Max	Median, Mean ± SD	Min, Max	Median, Mean ± SD	Min, Max	Median, Mean ± SD	Min, Max
0.1	54, 52 ± 13	14, 73	17, 18 ± 5	10, 26	146, 141 ± 32	42, 177	30, 34 ± 10	25, 53
0.2	46, 41 ± 18	2, 68	11, 13 ± 8	3, 27	126, 109 ± 47	9, 180	20, 25 ± 14	7, 50
0.3	41, 38 ± 14	1, 57	14, 15 ± 6	6, 24	126, 116 ± 38	6, 144	28, 30 ± 13	9, 51
0.4	36, 31 ± 14	2, 50	15, 14 ± 5	2, 20	110, 104 ± 41	7, 155	30, 31 ± 9	10, 49
0.5	35, 32 ± 12	1, 48	12, 12 ± 4	3, 19	121, 110 ± 37	4, 146	30, 28 ± 10	12, 46
1	25, 24 ± 8	2, 35	8, 8 ± 3	2, 13	99, 92 ± 29	11, 125	26, 25 ± 8	7, 35
2	17, 16 ± 5	2, 21	5, 4 ± 2	1, 8	70, 64 ± 20	9, 82	20, 18 ± 7	3, 26
3	12, 11 ± 4	1, 14	4, 4 ± 1	1, 6	49, 45 ± 15	5, 60	15, 15 ± 4	7, 20
4	10, 9 ± 2	1, 11	3, 3 ± 1	2, 4	40, 37 ± 8	8, 46	12, 12 ± 3	6, 16
5	8, 7 ± 2	2, 10	3, 3 ± 1	1, 4	32, 31 ± 7	8, 39	10, 10 ± 3	5, 15

Supplementary Table 8

Benchmarking of scaling impact on MoS_2 FETs
(parentheses show the number of devices used for the study)

	$\mu_{g_{\mathrm{m}}} (cm^2\, V^{-1} s^{-1})$			$I_{\mathrm{ON}} (\mu A .\, \mu m^{-1})$	
	Our work	[3]	[4]	Our work	[3]
L_{CH} (μm)	Median, Mean ± SD	Median, Mean ± SD	Median, Mean ± SD	Median, Mean ± SD	Median, Mean ± SD
0.1	3.6, 4 ± 1 (17)	3, 2.7 ± 0.9 (17)		100, 99 ± 23 (17)	39.6, 36.7 ± 14.2 (17)
0.2	7.2, 6.6 ± 3.1 (22)	5, 4.6 ± 1.7 (24)		87, 78± 33 (22)	28.4, 27.1 ± 12.2 (24)
0.3	9.5, 8.9 ± 3.7 (22)			79, 72 ± 25 (23)	
0.4	11.3, 9.1 ± 4.3 (23)			69, 59 ± 26 (23)	
0.5	11.7, 10.8 ± 5.1 (23)	9.2, 8.5 ± 3 (27)		66, 62 ± 22 (23)	25.1, 22.3 ± 10 (27)
1	14.7, 14.2 ± 5.4 (21)	11.1, 10.5 ± 3.4 (27)		49, 46 ± 15 (23)	12.1, 12.9 ± 5 (27)
2	19.3, 17.8 ± 7.3 (21)			32, 30 ± 10 (22)	
3	17.8, 20.1 ± 4 (15)			23, 21 ± 7 (19)	
4	22.5, 23.1 ± 3.6 (19)		Nil, 34.2 ± 3.6 (200) L_{CH} = 4-8.6 μm	19, 17 ± 4 (20)	
5	23.9, 24.2 ± 3.1 (17)			15, 14 ± 3 (19)	

Supplementary Figure 7

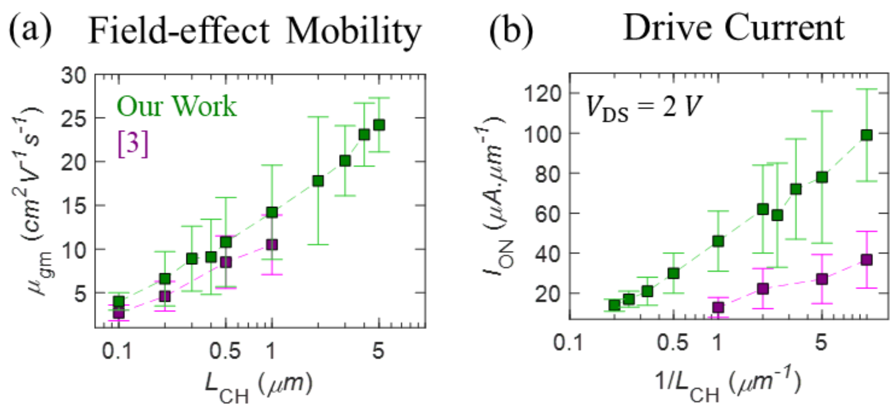

Supplementary Figure 7. Benchmarking scaling of MoS$_2$ FETs. Channel length dependent statistics with literature for a) field-effect mobility and b) drive current for synthetic monolayer MoS$_2$ FETs. Using error bar plots, mean and standard deviation is shown.

Supplementary Table 9

Device-to-device variation in saturation velocity				
	MoS$_2$		WS$_2$	
	Median, Mean ± SD	Min, Max	Median, Mean ± SD	Min, Max
v_{SAT} $(cm.sec^{-1})$ (10^5)	6.4, 5.9 ± 2.5	0.2, 11.2	4, 4.1 ± 1.5	1, 6.9

Supplementary References

[1] Q. Smets, B. Groven, M. Caymax, I. Radu, G. Arutchelvan, J. Jussot*, et al.*, "Ultra-scaled MOCVD MoS2 MOSFETs with 42nm contact pitch and 250µA/µm drain current," pp. 23.2.1-23.2.4, 2019.

[2] C. Min, T. Kamins, P. V. Voorde, C. Diaz, and W. Greene, "0.18-µm fully-depleted silicon-on-insulator MOSFET's," *IEEE Electron Device Letters,* vol. 18, pp. 251-253, 1997.

[3] H. Liu, M. Si, S. Najmaei, A. T. Neal, Y. Du, P. M. Ajayan*, et al.*, "Statistical study of deep submicron dual-gated field-effect transistors on monolayer chemical vapor deposition molybdenum disulfide films," *Nano Lett,* vol. 13, pp. 2640-6, Jun 12 2013.

[4] K. K. H. Smithe, S. V. Suryavanshi, M. Munoz Rojo, A. D. Tedjarati, and E. Pop, "Low Variability in Synthetic Monolayer MoS2 Devices," *ACS Nano,* vol. 11, pp. 8456-8463, Aug 22 2017.